Please cite this article in press as: Fitzmaurice et al., β-Barrel proteins dictate the effect of core oligosaccharide composition on outer membrane mechanics, Biophysical Journal (2025), https://doi.org/10.1016/j.bpj.2025.01.017

Biophysical Journal
Article

Biophysical Society

β-Barrel proteins dictate the effect of core oligosaccharide composition on outer membrane mechanics

Dylan R. Fitzmaurice,[1] Anthony Amador,[1] Tahj Starr,[1] Glen M. Hocky,[2] and Enrique R. Rojas[1,*]
[1]Department of Biology, New York University, New York, New York and [2]Department of Chemistry and Simons Center for Computational Physical Chemistry, New York University, New York, New York

ABSTRACT The outer membrane is the defining structure of Gram-negative bacteria. We previously demonstrated that it is a major load-bearing component of the cell envelope and is therefore critical to the mechanical robustness of the bacterial cell. Here, to determine the key molecules and moieties within the outer membrane that underlie its contribution to cell envelope mechanics, we measured cell-envelope stiffness across several sets of mutants with altered outer-membrane sugar content, protein content, and electric charge. To decouple outer membrane stiffness from total cell envelope stiffness, we developed a novel microfluidics-based "osmotic force-extension" assay. In tandem, we developed a method to increase throughput of microfluidics experiments by performing them on color-coded pools of mutants. We found that truncating the core oligosaccharide, deleting the β-barrel protein OmpA, or deleting lipoprotein outer membrane-cell wall linkers all had the same modest, convergent effect on total cell-envelope stiffness in *Escherichia coli*. However, these mutations had large, variable effects on the ability of the cell wall to transfer tension to the outer membrane during large hyperosmotic shocks. Surprisingly, altering the electric charge of lipid A had little effect on the mechanical properties of the envelope. Finally, the presence or absence of OmpA determined whether truncating the core oligosaccharide decreased or increased envelope stiffness (respectively), revealing sign epistasis between these components. Based on these data we propose a putative structural model in which the spatial interactions between lipopolysaccharides, β-barrel proteins, and phospholipids coordinately determine cell envelope stiffness.

SIGNIFICANCE The outer membrane is the defining cellular structure of Gram-negative bacteria, a group that contains many important pathogens such as *Escherichia coli*, *Vibrio cholerae*, and *Pseudomonas aeruginosa*. One role of the outer membrane is to block small molecules such as antibiotics. However, it is increasingly clear that it also functions as a structural exoskeleton that is critical for the cell's ability to cope with internal and external mechanical forces. Here, we carefully dissect the molecular basis for the load-bearing capacity of the outer membrane by screening a set of mutants with a new cell biophysics assay.

INTRODUCTION

The cell envelope of Gram-negative bacteria (Fig. 1 *A*) is a permeability barrier and exoskeleton that mediates all interactions between the cell and its environment, defines cell shape, and confers robust mechanical properties to the cell. This latter function is vital to bacteria during osmotic fluctuations (1), growth in confined spaces (2), and antibiotic exposure (3). The envelope is comprised of three essential layers: the plasma membrane, the peptidoglycan cell wall, and the outer membrane—an asymmetric bilayer with a phospholipid inner leaflet and a lipopolysaccharide outer leaflet (Fig. 1 *B*). Until recently, the mechanical properties of the cell envelope were exclusively attributed to the covalently crosslinked cell wall (4,5). However, we demonstrated that the outer membrane of *Escherichia coli* is actually more stiff than the cell wall with respect to surface tension in the cell envelope (1). Furthermore, several major genetic and chemical perturbations to the outer membrane dramatically reduced its stiffness, leading to cells that were highly vulnerable to lysis during antibiotic treatment or osmotic shocks, which lead to acute changes in the

Submitted September 24, 2024, and accepted for publication January 23, 2025.

*Correspondence: rojas@nyu.edu

Editor: Emma Sparr.
https://doi.org/10.1016/j.bpj.2025.01.017

Please cite this article in press as: Fitzmaurice et al., β-Barrel proteins dictate the effect of core oligosaccharide composition on outer membrane mechanics, Biophysical Journal (2025), https://doi.org/10.1016/j.bpj.2025.01.017

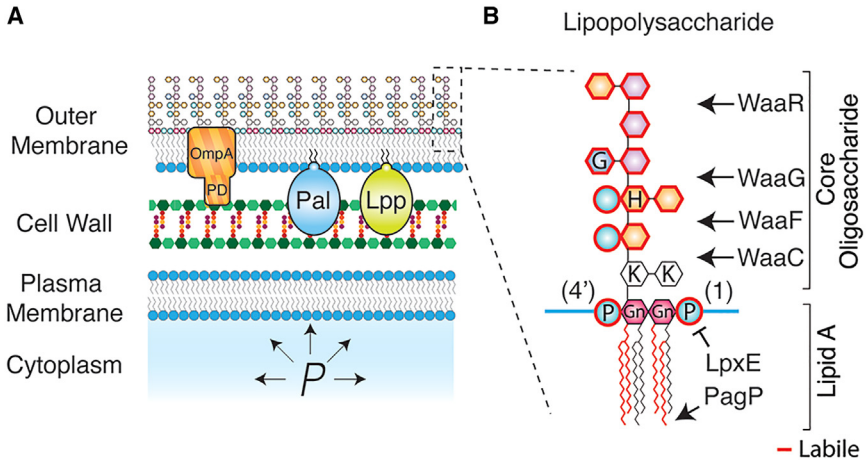

FIGURE 1 The Gram-negative cell envelope is complex. (*A*) Schematic of the Gram-negative cell envelope. PD, periplasmic domain of OmpA; *P*, turgor pressure. (*B*) Chemical structure of lipopolysaccharide with structure-modifying enzymes. Moieties outlined in red are enzymatically labile. Gn, glucosamine; P, phosphate; H, heptose; G, glucose; K, keto-deoxyoctulosonate.

hydrostatic pressure within the cell (the "turgor pressure," Fig. 1 *A*).

This discovery prompted three immediate questions: first, with respect to changes in turgor pressure, what are the constitutive mechanical properties of the outer membrane (e.g., linear versus nonlinear)? Second, are there key molecules or moieties that determine these properties, or do they emerge from the complex interactions of outer membrane components acting as a whole? Third, is there a specific architecture underlying how outer membrane components are connected that allows them to bear mechanical loads (e.g., "in series" or "in parallel")?

The intermolecular ionic bonds between the lipid A domains of lipopolysaccharides (Fig. 1 *B*) are, collectively, a leading candidate for a mechanical chassis within the outer membrane. Lipid A consists of an N-acetyl glucosamine dimer (the headgroup) linked to six acyl chains that interface with the inner leaflet of the outer membrane. The headgroup is phosphorylated at the 1 and 4′ carbons, which bind lipopolysaccharides to one another in the presence of divalent magnesium ions via intermolecular ionic "salt bridges" between phosphate groups (Fig. 1 *B*). These ionic bonds create a lipopolysaccharide-magnesium gel out of the outer membrane. Consistent with this model, outer membrane proteins exhibit highly constrained subdiffusive motion (6–8) and chelation of magnesium from the outer membrane results in a porous, weak outer membrane as would be expected if salt bridges were key load-bearing bonds (1). However, it is likely that magnesium chelation completely destabilizes the outer membrane, making it difficult to decouple the mechanical contributions of the salt bridges from those of other interactions that are also eliminated by this process. For example, mechanical forces could also be borne by hydrophobic interactions between the acyl moieties of lipid A, which are indirectly disrupted by magnesium chelation.

Bacteria can enzymatically modify lipid A, including its electrical charge, in response to environmental stimuli. For example, in response to weak acids *E. coli* ligates phosphoethanolamine and 4-aminoarabinose to lipid A phosphates, which makes it less anionic and results in increased outer membrane permeability (9). In principle, such modifications could also provide a way for bacteria to adaptively tune their mechanical properties if these properties were dependent, for example, on electric charge density. Practically, it is possible to controllably test the effect of lipid A modifications by ectopically expressing the specific enzymes that modify it (10).

Besides lipid A, lipopolysaccharides possess two polysaccharide moieties, which could also make mechanical contributions to the outer membrane. The core oligosaccharide is a 10-residue heteropolymer (Fig. 1 *B*) that is usually conserved within genera or families of Gram-negative bacteria (11). Core oligosaccharide synthesis occurs sequentially by the Waa monosaccharide transferases, such that the deletion of one of these enzymes results in an oligosaccharide that is truncated at the residue attached by that enzyme (Fig. 1 *B*). Undomesticated wild-type Gram-negative bacteria ligate an additional polysaccharide called the O-antigen to the terminal core-oligosaccharide residue; the composition of the O-antigen is highly variable across bacterial species and strains. Interestingly, the O-antigen can confer mechanical integrity to the cell envelope even if it is electrically neutral (1). Whether the specific length or composition of the core oligosaccharide also affects outer membrane stiffness is unknown; however, certain mutants with truncated core oligosaccharides (*ΔwaaC* and *ΔwaaG*; Fig. 1 *B*) exhibit increased outer membrane vesiculation (12), which may point to a weakened outer membrane.

In addition to lipopolysaccharides, the outer membrane is densely loaded with proteins (13). Most of these are β-barrel proteins: β-sheets that are folded into transmembrane cylinders by the Bam complex (14,15). Certain β-barrel proteins are selective molecular pores ("porins"). For example, OmpF and OmpC are highly abundant β-barrel porins in *E. coli* that regulate outer membrane permeability in

Please cite this article in press as: Fitzmaurice et al., β-Barrel proteins dictate the effect of core oligosaccharide composition on outer membrane mechanics, Biophysical Journal (2025), https://doi.org/10.1016/j.bpj.2025.01.017

response to extracellular osmolarity, while LamB mediates uptake of maltose (16,17). Whether these porins, generically, are also important for the mechanical integrity of the cell envelope is unknown. However, the structure and folding pattern of the β-barrel protein EspP is sensitive to tension in the outer membrane, providing insight into how these proteins could bear mechanical forces (18).

One β-barrel protein known to be critical for the mechanical integrity of the cell envelope is the highly abundant OmpA: the deletion of this protein causes drastic weakening of the outer membrane (1). However, as for the case of magnesium chelation it is unknown if this means that OmpA is a specific mechanical element or if its elimination causes global destabilization of the cell envelope. This question is particularly relevant to the case of OmpA since it possesses a periplasmic domain that specifically binds to the peptidoglycan cell wall (that is not present in other β-barrel proteins), making it likely that its deletion has pleiotropic effects on the global mechanical properties of the cell envelope.

OmpA is in fact one of three proteins that physically link the outer membrane to the cell wall (Fig. 1 *A*). The other two linkers, Pal and Lpp, are lipoproteins. Pal noncovalently binds the cell wall through a domain homologous to OmpA's periplasmic domain, and is critical for mediating constriction of the outer membrane during cell division (19,20). Lpp is covalently ligated to the cell wall and acts as a molecular pillar that determines the width of the periplasm (21,22). Collectively, OmpA, Pal, and Lpp prevent outer membrane vesiculation (23). We previously found that bacterial mutants lacking any of these proteins are highly susceptible to lysis upon repeated osmotic shocks (1). It is unknown, however, if these phenotypes are directly due to the load-bearing capacity of the proteins themselves or indirectly due to the decoupling of the outer membrane and cell wall that results from their deletion. Furthermore, it is unknown whether during modest osmotic shocks these molecular linkers are important for transferring mechanical forces between the cell wall and outer membrane.

Our previous assays for interrogating cell envelope mechanics were useful for highlighting the critical contribution of the outer membrane to total cell-envelope stiffness (1), but were limited due to issues of specificity and throughput. Furthermore, they did not provide information about the constitutive mechanical properties of the cell envelope. One assay we developed was a microfluidics "plasmolysis-lysis" experiment that estimated the ratio between the stiffnesses of the outer membrane, k_{om}, and the cell wall, $k_{\mathrm{cw}}{}^{1}$ (Fig. S1). In this assay, cells were subjected to a large (3 M) hyperosmotic shock and subsequently perfused with detergent, which caused cell lysis and dissolved the outer membrane. Although turgor pressure was completely depleted, we found that, after hyperosmotic shock (but before detergent perfusion), the cell wall was still stretched because of its association with the outer membrane, which prevented the wall from relaxing to its rest state by bearing in-plane surface compression (Fig. S1). By quantifying the contractions of the cell wall upon hyperosmotic shock and lysis—and treating the outer membrane and cell wall as parallel linear materials—we estimated k_{om}/k_{cw} (Eq. 1, materials and methods). For *E. coli*, we found that the outer membrane stiffness was approximately 1.5 times greater than cell wall stiffness. Furthermore, mutations that reduced this ratio sensitized bacteria to osmotic shocks and antibiotics. As a whole, this analysis pipeline provided a practical empirical quantification of cell-envelope mechanical properties. However, it did not alone decouple the stiffness of the outer membrane from that of the cell wall, which is particularly important for assessing pleiotropic effects of mutations to the outer membrane on the mechanical properties of the cell wall.

An important aspect of the plasmolysis-lysis assay is that for mutants with impaired connections between the outer membrane and the cell wall, the large hyperosmotic shock is likely to cause partial detachment of the outer membrane from the cell wall. If so, during this treatment the outer membrane will not be able to coordinately bear envelope tension with the cell wall, regardless of its intrinsic stiffness. As a result, the quantity k_{om}/k_{cw} that this assay reports is more accurately the ratio between the "effective outer membrane stiffness" and the stiffness of the cell wall.

In another assay, we probed cell-envelope mechanical properties by measuring cell-envelope deformation in response to a small hyperosmotic shock of a single magnitude ($\Delta C = 200$ mM) (1). This caused a defined reduction in turgor pressure ($\Delta P = -RT\Delta C$, where R is the ideal gas constant and T is the temperature) that partially deflated the cell. We demonstrated that the degree of this deformation was inversely related to the stiffness of the cell envelope. However, using a single shock magnitude did not provide the specific scaling relationship between envelope deformation and pressure changes (linear versus nonlinear). This information is important since the cell wall exhibits nonlinear strain-stiffening as measured via atomic force spectroscopy (24). If this behavior also occurs during osmotic shocks it would confound the meaning of deformation at a single shock magnitude.

Finally, all existing methodologies to measure cell-envelope mechanical properties at the single-cell level—including atomic force microscopy (24) and cell bending assays (25)—are relatively low-throughput, typically requiring several replicate experiments for each bacterial strain or mutant. This limits our ability to efficiently screen enough mutants to obtain a comprehensive understanding of the relationship between cell envelope composition and cell-envelope mechanical properties.

In sum, due to technical limitations we lack a deep understanding of the constitutive mechanical properties of the cell envelope, and how molecular components give rise to these properties. To address this, we developed a new "osmotic

Please cite this article in press as: Fitzmaurice et al., β-Barrel proteins dictate the effect of core oligosaccharide composition on outer membrane mechanics, Biophysical Journal (2025), https://doi.org/10.1016/j.bpj.2025.01.017

force-extension assay" to quantitatively measure cell-envelope stiffness (Fig. 2, *A–D*). Using this assay, we found that the cell envelope is a linear elastic material with respect to in-plane surface compression. In combination with the plasmolysis-lysis assay (Fig. S1), the osmotic force-extension assay also allowed us to decouple effective outer membrane stiffness from cell-wall stiffness. To accelerate throughput, we developed a method to color-code bacterial strains using combinations of nontoxic fluorophores so we could perform our microfluidics assays on pools of mutant bacteria (Fig. 3 *A*).

Using these assays, we systematically measured how genetic alterations of three families of molecules and moieties within the outer membrane—core oligosaccharides, β-barrel proteins, and lipid A—affect cell-envelope and outer membrane stiffness. A simple but important result of our analysis was that major perturbations to any of these components had the same quantitative effect on cell envelope stiffness, suggesting that this property emerges as a collective property of envelope components. We also found that, while systematic truncation of the core oligosaccharide of *E. coli* decreased cell-envelope and outer-membrane stiffness, the same mutations increased these properties in the absence of OmpA. Based on these results, we propose a putative model for how the interactions between β-barrel proteins, lipopolysaccharides, and phospholipids coordinately determine the mechanical properties of the cell envelope. As a whole, our analysis provides a more resolved picture of the mechanical infrastructure of the cell envelope than was possible with previous methods, and provides new broadly useful assays for interrogating this infrastructure.

MATERIALS AND METHODS

Bacterial strains and culture conditions

Bacterial strains and plasmids used in this study are listed in Table S1. Bacteria were grown in lysogeny broth (LB), Lennox formulation (5 g L^{-1} NaCl, Fisher Bioreagents, Waltham, MA) overnight in a rotary shaker at 37°C. For selection, 50 μg/mL kanamycin (Sigma-Aldrich, St. Louis, MO) or 100 μg/mL ampicillin (Sigma-Aldrich, St. Louis MO) were used. The osmolarity of the growth medium was modulated with D-Sorbitol (Sigma-Aldrich, St. Louis, MO) using the CellASIC ONIX microfluidic platform.

Construction of chromosomal gene deletion mutants

P1 vir phage transduction was used to move selectable deleted genes from the donor BW25113 strain to the recipient MG1655 strain (26). Mutations were confirmed by PCR using primers that anneal outside of flanking regions of the deleted gene (Table S2). When necessary, excision of the resistance gene was carried out using the helper plasmid pCP20 (27).

Lambda phage recombineering

To generate the mutant allele of *ompA* lacking the periplasmic domain ($\Delta ompA^{PD}$) lambda red recombineering was used. Cells carrying the red recombinase expression plasmid, pKD46, were grown in 30 mL LB with ampicillin at 30°C to an OD of 0.4. The culture was then inoculated with L-arabinose (Fisher Scientific, Waltham, MA) to a final concentration of 10% and incubated at 30°C for an additional 15 min. To make electrocompetent cells, the culture was initially chilled on ice and then washed twice with ice-cold ultrapure deionized water, and once with ice-cold 10% glycerol (Sigma-Aldrich, St. Louis, MO) in ultrapure deionized water. Electrocompetent cells were aliquoted into 30 μL suspensions and stored at −80°C. Electroporation was conducted with a Gene Pulser Xcell Electroporator (Bio-Rad, Hercules, CA) with 0.2 cm electrode gap cuvettes (Bio-Rad, Hercules, CA). Competent cells (30 μL) were inoculated with at least 200 ng of DNA, and shocked with a 2.5 kV voltage for 4 ms. Shocked cells were immediately

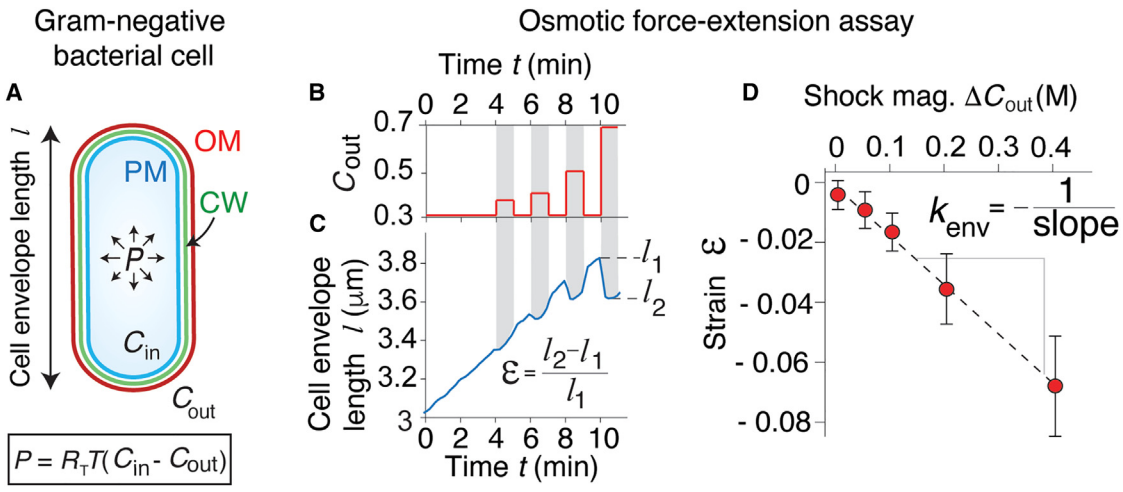

FIGURE 2 An osmotic force-extension assay measures total cell-envelope stiffness. (*A*) (*Top*) Diagram of a Gram-negative bacterial cell inflated with turgor pressure, *P*. OM, outer membrane; CW, cell wall; PM, plasma membrane; C_{in}, cytosolic osmolarity; C_{out}, osmolarity of the growth medium. (*Bottom*) Turgor pressure is proportional to the difference between the cytosolic and growth medium osmolarities, where R_T is the gas constant and T is the temperature. (*B*) Osmolarity of growth medium versus time during an osmotic force-extension experiment. (*C*) Cell-envelope length during an osmotic force-extension experiment. The duration of osmotic treatment is shaded gray. (*D*) Mechanical strain in cell length versus shock magnitude. The dotted line is the best fit using linear regression. Cell envelope stiffness, k_{env}, is calculated as the inverse of the slope of the regression. Error bars are ±1 SE from a single experiment on wild-type (BW25113) cells.

Please cite this article in press as: Fitzmaurice et al., β-Barrel proteins dictate the effect of core oligosaccharide composition on outer membrane mechanics, Biophysical Journal (2025), https://doi.org/10.1016/j.bpj.2025.01.017

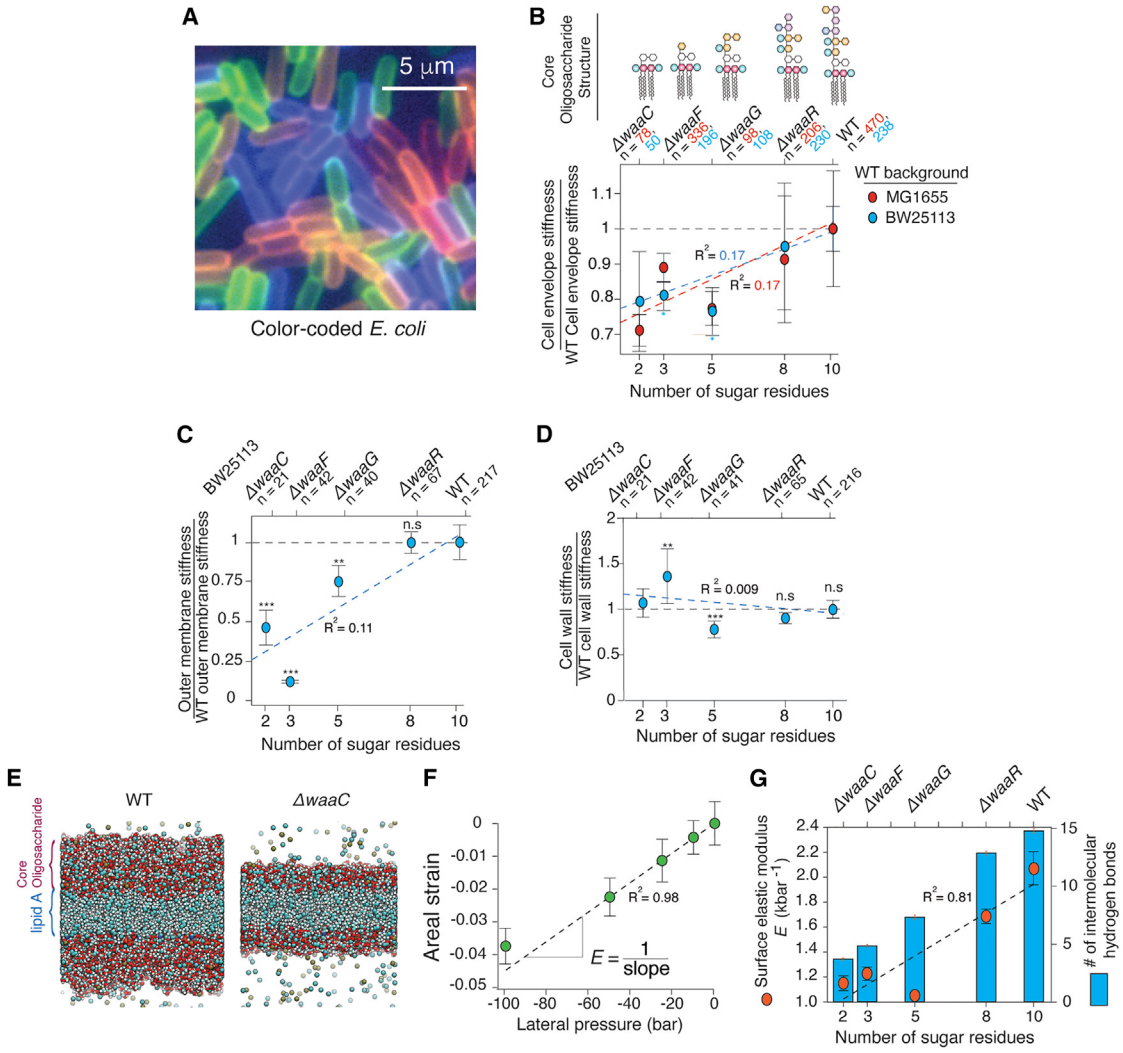

FIGURE 3 Cell envelope and outer membrane stiffness are proportional to lipopolysaccharide length. (*A*) A pool of color-coded *E. coli* cells. Scale bar is 5 μm. (*B*) Cell envelope stiffness versus core oligosaccharide length, normalized by wild-type cell-envelope stiffness for Δ*waaC*, Δ*waaF*, Δ*waaG*, Δ*waaR*, and wild-type cells in both the BW25113 and MG1655 parental backgrounds, respectively. Sample size (*n*) is listed for BW25113 (*blue*) and MG1655 (*red*) parental strains. Error bars indicate ±1 SD across 2–3 experiments per mutant. (*C*) Cell wall stiffness versus core oligosaccharide length, normalized to wild-type cell wall stiffness. (*D*) Outer membrane stiffness versus core oligosaccharide length, normalized to wild-type outer membrane stiffness. (*E–G*) Are results from MD simulations. (*E*) Illustration of simulated wild-type lipopolysaccharide bilayer (*left*) and *ΔwaaC* lipopolysaccharide bilayer (*right*). (*F*) Areal strain versus lateral pressure for the wild-type simulated lipopolysaccharide bilayer. (*G*) (*Left y* axis, *orange circles*). Surface (2D) elastic modulus for simulated Δ*waaC*, Δ*waaF*, Δ*waaG*, Δ*waaR*, and wild-type lipopolysaccharide bilayers. Error bars indicate ±1 SE from the linear regression of strain versus pressure. (*Right y* axis, *blue bars*) Mean number of hydrogen bonds between core-oligosaccharides for simulated Δ*waaC*, Δ*waaF*, Δ*waaG*, Δ*waaR*, and wild-type lipopolysaccharide bilayers. Sample size (*n*) is listed for all cells. ns, nonsignificant; **p* > 0.05, ***p* > 0.01, ****p* > 0.001.

recovered with 1 mL Super Optimal Broth (SOC medium, Sigma-Aldrich, St. Louis, MO) and incubated with shaking at 30°C for 2 h. Next, 500 μL of transformant culture was spun down, resuspended in 100 μL LB, and spread onto agar plates. Plates were incubated overnight at 37°C and kanamycin-resistant transformants were selected the following day.

To delete the periplasmic domain, the kanamycin cassette, which included FRT sites, was first amplified from pKD13 using Primers TS023 and TS024 (Table S2). The amplicon was used as a template for PCR with primers AA003 and AA004, which added the final 50 bp of *ompA*'s β-barrel domain to the 5′-terminus of the kanamycin cassette and the 50 bp downstream of *ompA*'s stop codon to the 3′-terminus of the cassette. The product of this reaction was treated with DpnI (New England Biolabs, Ipswich, MA) for 2 h at 37°C, followed by column purification (QIAquick PCR Purification Kit, QIAGEN, Hilden, Germany). The purified, linear DNA was used for electroporation of BW25113 cells carrying the red recombinase expression plasmid, pKD46, following the protocol described above. After primary selection, P1 vir phage transduction was used to move the truncated *ompA* gene with kanamycin resistance into the recipient MG1655 background. Chromosomal integration of $\Delta ompA^{PD}$::*kan* was verified through colony PCR using primer pairs AA001/TS025 and AA002/TS026 followed by sequencing of the PCR product.

Imaging in microfluidic devices

Cells were imaged on a Nikon Eclipse Ti-E inverted fluorescence microscope with a 100× (NA 1.45) oil-immersion objective. For all experiments we used CellASIC B04A microfluidic perfusion plates, and medium was exchanged

Please cite this article in press as: Fitzmaurice et al., β-Barrel proteins dictate the effect of core oligosaccharide composition on outer membrane mechanics, Biophysical Journal (2025), https://doi.org/10.1016/j.bpj.2025.01.017

using the CellASIC ONIX microfluidic platform. Images were collected on a sCMOS camera (Prime BSI). Experiments were performed at 37°C in a controlled environmental chamber (HaisonTech, Taipei, Taiwan).

Combinatorial color coding

To accelerate our screen for the effect of genetic perturbations on cell envelope stiffness, multiple bacterial strains were color-coded with nontoxic dyes (Fig. S2), pooled, and experiments were performed on the pool. The color code was then decoded using custom computational image analysis (Fig. S2). The dyes used to color-code bacteria were: fluorescent D-amino acid HADA (Tocris Bioscience, Bristol, United Kingdom), MitoTracker Orange CM-H_2TMRos (Invitrogen, Waltham, MA), MitoView Green (Biotium, Fremont, CA), MitoView 720 (Biotium, Fremont, CA). Stock solutions of 100 mM HADA, 500 μM MitoTracker Orange CM-H_2TMRos, 200 μM MitoView Green, and 200 μM MitoView 720 were used. HADA is covalently incorporated into the cell wall, whereas the MitoView dyes noncovalently label the plasma membrane. For concentrated stock solutions, all dyes were dissolved in DMSO. The dyes or combinations thereof did not affect cell-envelope stiffness (Fig. S7). Using four dyes of different colors, we could successfully pool up to 10 strains at once; however, we typically pooled 3–4 strains per experiment. To control for technical experiment-to-experiment variability we included the isogenic wild-type strain in each pool of mutants that we measured, and we also performed experiments in triplicate and permuted the dye combinations used to label the pooled strains.

For color coding, MitoTracker Orange (250 nM final concentration), MitoView Green (200 nM final concentration), and MitoView 720 (100 nM final concentration) were added to exponential-phase cultures 30 min before pooling strains. HADA (250 μM final concentration) was added to exponential phase cultures 1 h before pooling. Dyed cells were back-diluted 200× into LB (without dye) and were then immediately loaded into the microfluidic device.

Osmotic force-extension assay

Overnight cultures were diluted 100-fold into 1 mL of fresh LB and incubated for 2 h with shaking at 37°C. During this incubation, dyes for color coding were added at the times given above. Plates were loaded with medium and prewarmed to 37°C. Alexa Fluor 647 NHS Ester (Thermo Fisher Scientific, Waltham, MA) (5 μg/mL) dye was added to specific medium as a tracer dye to monitor medium switching.

Color-coded cells were pooled and loaded into the loading well of the microfluidic plate. After loading them into the perfusion chamber, cells were grown for 5 min in LB in the imaging chamber before being subjected to a series of hyperosmotic shocks in LB supplemented with 50, 100, 200, and 400 mM sorbitol for 1 min each. Between shocks the medium was switched back to LB for 1 min.

To calculate the amplitude of length oscillations during osmotic shocks, cells were tracked using custom MATLAB algorithms. First, cell-envelope length (l) was automatically computed and the elongation rate ($\dot{e} = \frac{d \ln l}{dt}$) was calculated for each cell. The effective population-averaged length was calculated by integrating the population-averaged elongation rate over time (28). The mechanical strain in cell envelope length caused by each hyperosmotic shock ($\varepsilon = \frac{l_1 - l_2}{l_2}$) was then calculated. Linear regression of mechanical strain as a function of shock magnitude was calculated where cell-envelope stiffness was defined as the inverse of the slope of the regression. Uncertainty was estimated using the standard error of the linear regression.

To control for experiment-to-experiment variability due to heterogeneity in microfluidic chips, we normalized cell-envelope stiffness to the internal wild-type control in each experiment before averaging across experiments.

Analysis code is available at: https://github.com/hocky-research-group/Fitzmaurice-OuterMembrane-2025.

Plasmolysis-lysis experiments

Plasmolysis-lysis experiments were performed as described previously (1), with minor changes. In brief, overnight cultures were diluted 100-fold into 1 mL of fresh LB medium and incubated with shaking at 37°C for 1 h. HADA (250 μM) was added to the culture and cells were incubated for an additional hour. Cultures were then back diluted 100-fold into 1 mL of prewarmed LB with 250 μM of HADA, which we added directly to the loading well of the microfluidic chip. After loading cells into the imaging chamber, they were perfused with LB for 5 min, followed by LB + 3 M sorbitol for 5 min, then with LB + 3 M sorbitol + 20% *N*-lauroyl sarcosine sodium salt (Sigma-Aldrich, St. Louis, MO) for 30 min, and finally with LB for 20 min. We measured the cell wall length upon lysis after this last step. One microliter of Alexa Fluor 647 NHS Ester dye (1 mg/mL) was added to every other perfusion well as a tracer dye to track media switching. A time-lapse image with a 10 s frame rate was taken during the initial 5 min period when the cells were perfused with LB. To avoid photobleaching of HADA and phototoxicity, a single image was taken during each of the next two perfusion periods when the cells were plasmolyzed (LB + 3 M sorbitol) and detergent-lysed (LB + 3 M sorbitol + *N*-lauroylsarcosine sodium salt), respectively.

The outer membrane and the cell wall were treated as parallel linear springs and the relative stiffnesses were calculated as:

$$\frac{k_{om}}{k_{cw}} = \frac{\varepsilon_l}{\varepsilon_p(\varepsilon_l + 1)} \tag{1}$$

where ε_p is the strain induced in the cell wall upon plasmolysis with 3 M sorbitol and ε_l is the additional strain induced by the detergent lysis of the cell (Fig. S1). By further substituting the total envelope stiffness ($k_{tot} = k_{cw} + k_{om}$) into Eq. 1, the stiffnesses of the cell wall and outer membrane were explicitly solved for in terms of experimentally measurable quantities:

$$k_{om} = \frac{k_{tot}}{1 + \frac{\varepsilon_p(\varepsilon_l + 1)}{\varepsilon_l}} \tag{2}$$

$$k_{cw} = \frac{k_{tot}}{1 + \frac{\varepsilon_l}{\varepsilon_p(\varepsilon_l + 1)}} \tag{3}$$

Outer membrane bulging experiments

For cell bulging experiments, the outer membrane was labeled with WGA-AF488 (ThermoFisher Scientific, Waltham, MA), which was added to the loading well to a final concentration of 10 μg/mL.

Molecular dynamic simulations

E. coli (K12) outer membrane models were built with five distinct lipopolysaccharide cores corresponding to the forms produced by *ΔwaaC*, *ΔwaaF*, *ΔwaaG*, *ΔwaaR*, and wild-type (Fig. 1 *B*), using the CHARMM-GUI online server (29) with CHARMM36 force field parameters (30,31) and TIP3P water. Symmetric lipopolysaccharide bilayers were generated to probe only the contribution of this molecule to the outer membrane. *ΔwaaC*, *ΔwaaR*, and wild-type simulated bilayers contained 53 LPS molecules on both the outer and inner leaflets, whereas *ΔwaaF*, *ΔwaaG* consisted of 55 LPS molecules where 22 had phosphate groups on Heptose 1 and 33 did not, to simulate experimental data (32). The minimum water height on the top and bottom of the system was set to 40 Å. Systems were minimized and equilibrated using the CHARMM-GUI lipids protocol (29). Production simulations were performed at 310.15 K in NPT using the Nosé-Hoover thermostat and barostat.

Please cite this article in press as: Fitzmaurice et al., β-Barrel proteins dictate the effect of core oligosaccharide composition on outer membrane mechanics, Biophysical Journal (2025), https://doi.org/10.1016/j.bpj.2025.01.017

Production data were collected using GROMACS 2020.4 molecular dynamics (MD) engine (33) patched with PLUMED version 2.7.0 (34). Lipopolysaccharide bilayers were run for 300 ns using a 2 fs timestep at lateral pressure $P = 0$ for an initial equilibration after which the pressure was changed to either 10, 25, 50, or 100 bar and run for an additional 300 ns.

Files for MD simulation setup and production runs are available: https://github.com/hocky-research-group/Fitzmaurice-OuterMembrane-2025.

Statistics

For osmotic force-extension assays, one-tailed *t*-tests were preformed to determine significance. The *t* stat was calculated as:

$$t - stat = \frac{(Stiffness_1 - Stiffness_2)}{sqrt\left(\frac{\sigma_1^2}{n_1} + \frac{\sigma_2^2}{n_2}\right)}$$

where σ is the standard deviation and *n* is the number of technical replicates. The degrees of freedom (*df*) were calculated as $n_1 + n_2 - 2$.

The *p* value was calculated using MATLAB's Student's *t* cumulative distribution function *tcdf* as:

$$p\ value = (1 - tcdf(t - stat, df))$$

Statistics for the plasmolysis-lysis assay and solving for outer membrane or cell wall stiffness alone, two-sample *t*-tests were used. The normalized k_{ratio}, k_{om}, or k_{cw} for single cells across experiments was compared between two samples, typically wild-type and mutant strains. The two-sample *t*-test was performed using the MATLAB's function *ttest2*.

For outer membrane bulging experiments χ^2 was performed using counts of single cells, which either did or did not bulge after hypoosmotic shock. *p* values were calculated using MATLAB's function *crosstab*.

RESULTS

An osmotic force-extension assay precisely measures cell envelope stiffness

Our goals were to develop a precise and efficient method for measuring the constitutive mechanical properties of the cell envelope, to decouple the stiffness of the outer membrane from the cell wall, and to apply these methods to a range of genetic mutations (and combinations thereof) to dissect the mechanical structure of the cell envelope. To begin, we developed a new "osmotic force-extension" assay (Fig. 2, *A–D*) in which we subjected cells to a series of hyperosmotic shocks of increasing magnitude, and measured the resulting contractions of the cell envelope (mechanical strain in cell length) caused by each shock (Fig. 2, *B* and *C*). We discovered that the dependence of strain on shock magnitude was precisely linear for shocks up to 400 mM, which allowed us to empirically define cell envelope stiffness, k_{env}, as the inverse of the slope of this dependence (Fig. 2 *D*). This result validated the treatment of the cell wall and outer membrane as linear springs in the plasmolysis-lysis assay (1). Therefore, by combining the two assays we could empirically solve for the stiffnesses of the cell wall and outer membrane in terms of experimentally measurable quantities (materials and methods, Eqs. 2 and 3).

To accelerate the throughput of this analysis pipeline we invented a technique to color-code bacterial strains with combinations of nontoxic fluorophores (Figs. 3 *A* and S2). This allowed us to pool up to 10 color-coded mutants and perform our microscopy/microfluidics assays on the pool at once (Fig. S2). An additional benefit of this method is that we could include the isogenic wild-type background in each pool of mutants, thereby providing an internal control for experiment-to-experiment variability in all experiments.

Cell envelope stiffness is correlated with core oligosaccharide length

We first used our analysis pipeline to measure the effects of truncations to the core oligosaccharide on the mechanical properties of the *E. coli* outer membrane. Because of the large contribution of the outer membrane to envelope stiffness, we hypothesized that even minor alterations to the core oligosaccharide would meaningfully affect global envelope stiffness. When we interrogated a set of mutants with deletions of the *waa* genes (Fig. 1 *C*), we found that total envelope stiffness was strongly correlated with core oligosaccharide length across two wild-type backgrounds of *E. coli* (Fig. 3 *B*). Furthermore, this dependence arose directly from weakening of the outer membrane (Fig. 3 *C*), whereas the stiffness of the cell wall did not depend on core oligosaccharide length (Fig. 3 *D*). Complete removal of the "outer core" (by deletion of *waaC*) leaving only the essential "inner core," resulted in a 20–30% reduction in total cell envelope stiffness (Figs. 3 *B* and S3) and a ≈60% reduction in effective outer membrane stiffness (Fig. 3 *C*). In contrast to *waa* mutants in the BW25113 wild-type background, most of the equivalent mutants in the MG1655 background lysed when we subjected them to our plasmolysis-lysis assay, therefore we could not decouple their outer membrane stiffness from their cell wall stiffness. However, the lysis underscores the strong effect that the truncations have on the mechanical integrity of the cell envelope.

Truncation of lipopolysaccharides may have pleiotropic effects on outer membrane composition. For example, deletion of *waaC* results in reduced expression of the major outer membrane porin OmpF (35). To test the effect of lipopolysaccharide truncation on outer membrane mechanics independent of pleiotropy, we used computational molecular dynamics simulations. In these simulations we subjected an all-atom model of the outer membrane to negative lateral pressure, characteristic of the mechanical forces experienced by the outer membrane during our experiments (Fig. 3 *E*). To isolate the mechanical contribution of lipopolysaccharides from that of phospholipids, we simulated symmetric lipopolysaccharide bilayers. Although this simplistic membrane will not predict absolute outer membrane stiffness, we reasoned that it would reveal the same

Please cite this article in press as: Fitzmaurice et al., β-Barrel proteins dictate the effect of core oligosaccharide composition on outer membrane mechanics, Biophysical Journal (2025), https://doi.org/10.1016/j.bpj.2025.01.017

quantitative relationships between core oligosaccharide length and outer membrane stiffness as our experimental data while avoiding the technical challenges of establishing a more realistic asymmetric system in silico.

We found that the dependence of areal strain on lateral pressure was approximately linear for compressions up to 5% (Fig. 3 *F*) and we thus empirically defined the surface elastic modulus, *E*, as the inverse of the slope of this dependence. Overall, truncations to the core oligosaccharide resulted in a decrease in the surface elastic modulus that was strikingly similar to the experimental dependence of cell-envelope stiffness on these truncations (compare Fig. 3, *G–B*).

By inspecting our experimental data in concert with our simulations, we inferred the relative importance of hydrogen bonds versus salt bridges in determining cell envelope and outer membrane stiffness. Deletion of *waaR*, which results in the removal of the two terminal sugar residues (accounting for ≈2 hydrogen bonds between core oligosaccharides) resulted in small decreases in experimental cell-envelope stiffness (Fig. 3 *B*) and in silico surface elastic modulus (Fig. 3 *G*), but had no measurable effect on outer membrane stiffness. On the other hand, deletion of *waaG*, which removes three more sugar residues that account for ≈5 hydrogen bonds, but also prevents phosphorylation of one of the remaining core oligosaccharides (32), resulted in a ≈25% reduction in both envelope and outer membrane stiffness (Fig. 3, *B* and *C*) and a ≈50% reduction in the elastic modulus of our simulated membrane (Fig. 3 *G*). The quantitative overestimate of the simulations may be due to the symmetry of this system since alterations to the core oligosaccharides will affect both bilayers (Fig. 3 *E*). Deletion of *waaF*, which removes one additional sugar residue and ≈2 hydrogen bonds (compared to *ΔwaaG*) had little effect on cell-envelope stiffness and surface elastic modulus but almost completely eliminated the effective contribution of the outer membrane to cell envelope stiffness during the plasmolysis-lysis assay (Fig. 3 *C*). We speculate that this mutation completely inhibits phosphorylation of the core oligosaccharide, which weakens the outer membrane and therefore limits its ability to bind tightly to the cell wall. Removal of the core oligosaccharide (including its salt bridges; Fig. S4) resulted in a 60% reduction in surface elastic modulus of the simulated outer membrane (Fig. 3 *G*), in quantitative agreement with the effect of *waaC* deletion on our experimental measurement of outer membrane stiffness. Together, our data suggest that both hydrogen bonds and salt bridges contribute commensurately to cell envelope mechanics, but that elimination of individual salt bridges causes particularly acute destabilization of the outer membrane.

The β-barrel and periplasmic domains of OmpA contribute to cell-envelope stiffness independently

We next used our experimental assays to measure how genetic perturbations to β-barrel proteins affected cell-envelope mechanical properties. We focused on OmpA so we could also interrogate the relative contributions of the β-barrel and periplasmic domains (Fig. 1 *A*). Therefore, we first measured the effect of deleting the entire protein (*ΔompA*) on cell-envelope stiffness, and then tested the effect of deletion of the periplasmic domain alone ($\Delta ompA^{PD}$).

When we subjected *ΔompA* mutants from three wild-type backgrounds to the osmotic force-extension assay, we found that this mutation resulted in a consistent ≈25% reduction in cell envelope stiffness (Fig. 4 *A*). Removing only the periplasmic domain had a quantitatively similar effect on envelope stiffness, suggesting that the periplasmic linker function rather than the β-barrel domain underlies OmpA's mechanical contribution. However, as in our previous study (1), we found that deletion of OmpA completely abolished the outer membrane's contribution to envelope stiffness in the plasmolysis-lysis assay. As a result, the effective outer membrane stiffness we measured was close to zero (Fig. 4 *B*). Interestingly, when we expressed only the linker-less β-barrel domain of OmpA, this partially restored outer membrane stiffness. While these results are consistent with the periplasmic linker being a key mechanical linchpin within the cell envelope, they also clearly demonstrate that the β-barrel alone contributes to outer membrane stiffness during large osmotic shocks.

One way that OmpA's β-barrel could contribute to the effective outer membrane stiffness during the plasmolysis-lysis assay but not to cell-envelope stiffness during the osmotic force-extension assay is by influencing the attachment of the outer membrane to the cell wall. To test this, we labeled the outer membrane and explicitly measured its deformation during intermediate (400 mM) hyperosmotic shocks, which partially deplete pressure. We found that, whereas the outer membrane of wild-type cells remained evenly attached to the cell wall, in a fraction of *ΔompA* mutant cells the hyperosmotic shock caused bulging of the outer membrane (Fig. 4, *C* and *D*). These outer membrane bulges were reminiscent of those observed previously upon vancomycin treatment (36). Surprisingly, expressing the β-barrel domain of OmpA alone suppressed the bulging phenotype. That is, the OmpA β-barrel prevents bulging of the outer membrane independent of its periplasmic linker, whereas the deletion of the linker did not promote bulging. One possible explanation for these observations is that the OmpA β-barrel meaningfully increases the bending stiffness of the outer membrane, thereby preventing bulging so long as Pal and Lpp are present to mediate connections between the cell wall and outer membrane.

To sum, our data paint a complex picture of OmpA's contribution to outer membrane mechanics. Deletion of the periplasmic linker is enough to modestly reduce envelope stiffness, to greatly reduce (effective) outer membrane stiffness, but not enough to prevent Pal and Lpp from holding the outer membrane and cell wall together. However,

Please cite this article in press as: Fitzmaurice et al., β-Barrel proteins dictate the effect of core oligosaccharide composition on outer membrane mechanics, Biophysical Journal (2025), https://doi.org/10.1016/j.bpj.2025.01.017

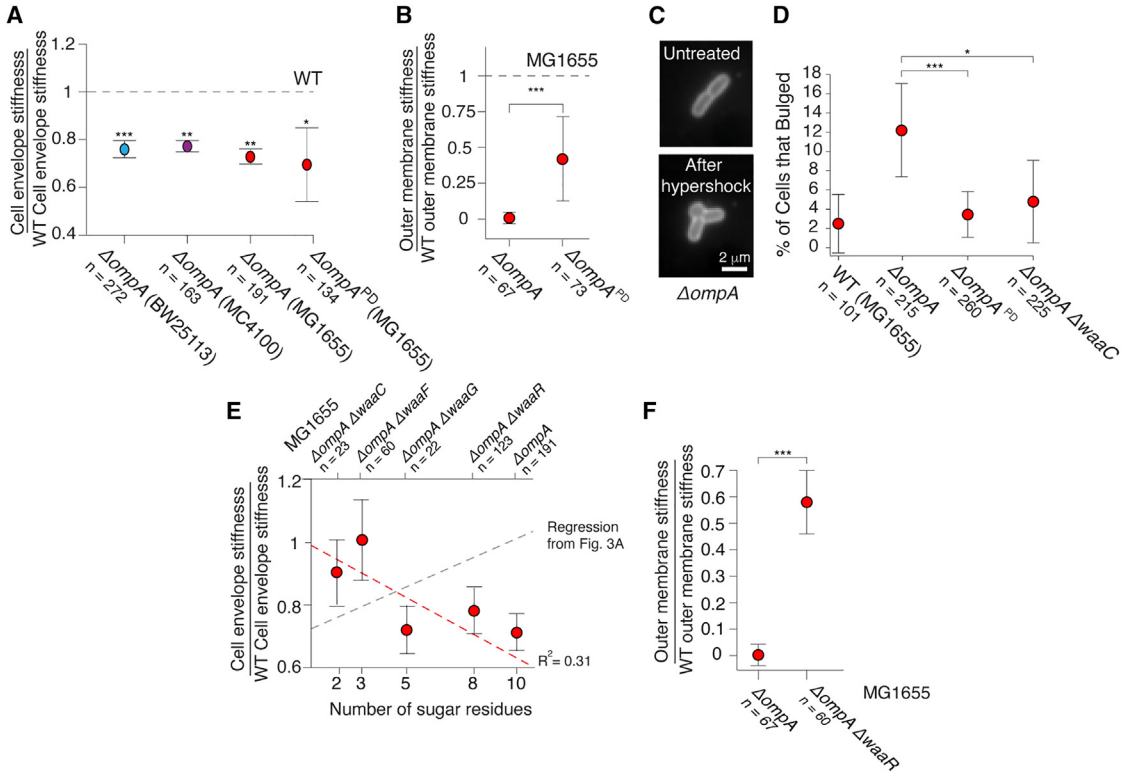

FIGURE 4 Mutations to *ompA* and *waa* genes exhibit sign epistasis. (*A*) Cell envelope stiffness for *ΔompA* mutants from three wild-type backgrounds, and for the deletion of the periplasmic domain (*ΔompA*^{PD}) of OmpA in the MG1655 background. (*B*) Outer membrane stiffness for the *ΔompA* and *ΔompA*^{PD} mutants. (*C*) A *ΔompA* cell before and after 400 mM hyperosmotic shock. Scale bar is 2 μm. *D*) Percentage of cells that developed outer membrane bulges after 400 mM hyperosmotic shocks. (*E*) Cell envelope stiffness versus core oligosaccharide length for mutants in a *ΔompA* background, normalized by wild-type cell-envelope stiffness. (*F*) Outer membrane stiffness for *ΔompA* and *ΔompA ΔwaaR* mutants. (*A, D,* and *E*) Error bars indicate ±1 SD across 2–3 experiments per mutant. (*B* and *F*) Error bars indicate ±1 SE across sample size (*n*) listed. Sample size (*n*) is listed for all cells. ns, nonsignificant; $*p > 0.05$, $**p > 0.01$, $***p > 0.001$.

additional deletion of the β-barrel domain is enough to loosen the attachment of the outer membrane to the cell wall and completely eliminate the effective contribution of the outer membrane to envelope mechanics during large hyperosmotic shocks (3 M) but not enough to weaken its contribution during modest ones (400 mM).

Mutations to core oligosaccharides and OmpA exhibit sign epistasis

We next examined how genetic interactions between mutation of the core oligosaccharides and mutation of OmpA affected cell-envelope mechanical properties. We reasoned that nonadditive effects of these combinations on stiffness would reveal genetic or structural interactions between core oligosaccharides and proteins. Surprisingly, we found that, while truncating the core oligosaccharide predictably decreased cell-envelope and outer-membrane stiffness in the presence of OmpA (Fig. 3 *B*), the same truncations increased cell envelope stiffness in the absence of OmpA (Fig. 4 *E*). Furthermore, deletion of *waaC* suppressed the outer membrane bulging upon hyperosmotic shock caused by deletion of *ompA*. However, 56% of *ΔompA ΔwaaC* mutant cells generated long outer membrane tethers upon hyperosmotic shock treatment (Fig. S5).

All but one of the *ΔompA Δwaa* double mutants lysed upon large hyperosmotic shock during the plasmolysis-lysis assay, therefore, we could not specifically decouple outer membrane stiffness for these strains. However, for the one double mutant that did survive (*ΔompA ΔwaaR*, which possessed the smallest perturbation to the core oligosaccharide) we found that truncation of the core oligosaccharide greatly increased the contribution of the outer membrane to cell envelope stiffness compared to the single *ΔompA* deletion (Fig. 4 *F*).

Collectively our data demonstrate that mutations of *ompA* and the *waa* genes result in what geneticists refer to as sign-epistasis, where the presence or absence of one gene determines the sign of the effect of a second gene on a given phenotype (37). Further research is required to understand the detailed molecular basis for this phenomenon, but based on our data we propose a simple putative model in which favorable interactions between β-barrel proteins and lipopolysaccharides stabilize the outer membrane and unfavorable interactions between phospholipids and lipopolysaccharides destabilize it (see discussion).

Please cite this article in press as: Fitzmaurice et al., β-Barrel proteins dictate the effect of core oligosaccharide composition on outer membrane mechanics, Biophysical Journal (2025), https://doi.org/10.1016/j.bpj.2025.01.017

Mutants of outer membrane-cell wall linkers phenocopy Δ*ompA* in envelope stiffness but not outer membrane stiffness

We next measured the effect of deletion of Lpp and Pal on cell envelope stiffness. Interestingly, we found that eliminating Lpp reduced total cell-envelope stiffness to precisely the same degree as eliminating OmpA or its periplasmic domain (Figs. 4 *A* and 5 *A*). Similarly, deletion of Lpp caused a reduction in outer membrane stiffness similar to that caused by deletion of OmpA's periplasmic domain but less than the deletion of the entire OmpA protein (Figs. 4 *C* and 5 *B*). We propose that the precise quantitative correspondence between these mutations means that they are effectively leading to a convergent, modest structural collapse of the cell envelope that does not depend on the structure or copy number of the protein that was eliminated. This implies that there is a threshold of outer membrane-cell wall connections that are required to prevent this collapse.

Compared with OmpA and Lpp, elimination of Pal caused a greater reduction of cell envelope stiffness and a much more dramatic effect on effective outer membrane stiffness (Fig. 5 *A* and *B*). In fact, during the plasmoysis-lysis assay, when cells were treated with detergent after having been plasmolyzed (Fig. S1), the cell wall elongated instead of contracting, leading to negative values of outer membrane stiffness (Fig. 5 *B*). The meaning of this is unclear, but one possibility is that in this mutant, the protoplast (plasma membrane and cytoplasm) can exert negative pressure on the cell envelope during plasmolysis, and because the outer membrane-cell wall links are severely undermined, the cell wall contracts below its rest length. Regardless, from these measurements we conclude that Pal is the most important of the three linkers mechanically.

Modifications to lipid A have weak effects on cell envelope stiffness

Our analysis demonstrated that hydrogen bonds and salt bridges between the core oligosaccharides bear force within the outer membrane. However, truncations to the core oligosaccharide require deletion of one of the *waa* genes and are not viewed as adaptive except when cells are subjected to strong selective pressure such lytic bacteriophage predation (38). Furthermore, most wild-type bacteria possess an O-antigen (which can also bear force (1)), precluding phenotypic adaptation via modulation of core oligosaccharide length. On the other hand, it is well understood that bacteria use a suite of enzymes to adaptively modify lipid A in response to environmental cues (9). By combinatorially expressing these enzymes (LpxE, LpxF, LpxO, LpxR, PagL, PagP) this adaptation was previously exploited to synthetically engineer *E. coli* to homogenously express specific variants of lipid A (10). For us, these mutants provided an opportunity to investigate the dependence of cell-envelope mechanics on lipid A chemistry and to explore whether, in principle, this chemistry could be used to mechanically adapt to their environment.

The control strain (BN1: W3110 *ΔlpxT ΔeptA ΔpagP*) homogenously expressed hexaacylated, bis-phosphorylated lipid A (Fig. 1 *B*), which is the most abundant species of lipid A in wild-type *E. coli* (10). We hypothesized that reducing the negative charge of the headgroup would reduce outer membrane stiffness. Surprisingly, when we removed the 1-phosphate group, the stiffness of the total cell envelope was unaffected and the effective stiffness of the outer membrane increased modestly (Fig. S6). Similarly, adding an acyl chain had little effect on cell envelope or outer membrane mechanical properties (Fig. S6).

DISCUSSION

We developed a new quantitative assay to empirically calculate the stiffness of the bacterial cell envelope. Cells were subjected to a series of hyperosmotic shocks of increasing magnitude, and the contraction of cell envelope length was measured. A simple but important result from this experiment was that the degree of contraction was linearly proportional to shock magnitude, allowing us to unambiguously define envelope stiffness (Fig. 2 *D*). This

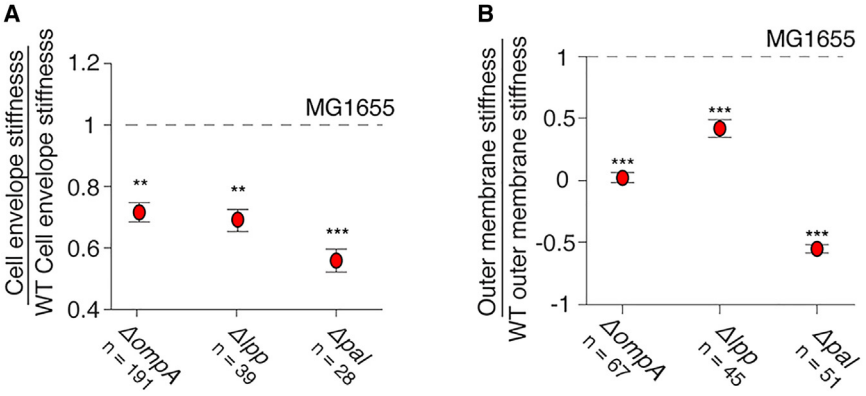

FIGURE 5 Deletion of Pal has a dramatic effect on cell envelope integrity. (*A*) Cell envelope stiffness of mutants for outer membrane-cell wall linkers. Error bars indicate ±1 SD across 3 experiments per mutant. (*B*) Outer membrane stiffness of mutants for outer membrane-cell wall linkers. Error bars indicate ±1 SE across sample size (*n*) listed. Sample size (*n*) is listed for all cells. ns, nonsignificant; $*p > 0.05$, $**p > 0.01$, $***p > 0.001$.

Please cite this article in press as: Fitzmaurice et al., β-Barrel proteins dictate the effect of core oligosaccharide composition on outer membrane mechanics, Biophysical Journal (2025), https://doi.org/10.1016/j.bpj.2025.01.017

result superficially contradicts previous AFM-based measurements of nonlinear mechanical properties of the cell wall (24). However, AFM deforms the cell envelope via indentation, causing stretching of the envelope rather than compression. We hypothesize that we would see similar nonlinear strain-stiffening if we could controllably perform our assay using hypoosmotic shocks instead of hyperosmotic shocks. In fact, we previously noted that hypoosmotic shocks cause negligible swelling of the envelope of cells during steady-state growth (39). This could reflect extreme strain-stiffening; however, it is difficult to control for the effect of stretch-activated ion channels (39), which decrease pressure upon hypoosmotic shocks and would therefore reduce cell envelope swelling. Therefore, we conclude that the cell envelope is linearly elastic for pressures up to the steady-state pressure at which cells grow. Interestingly, our initial applications of the osmotic force-extension assay to Gram-positive bacteria reveal that it is also linear elastic with respect to length deformation but not width deformation (40).

A second central finding of our study is that the core oligosaccharide moieties of lipopolysaccharides only contribute to cell envelope stiffness if the outer membrane possesses its full complement of β-barrel proteins. These proteins are densely packed in the outer membrane (13) and, in this light, lipopolysaccharides function as "mortar" that coats β-barrels and fills the areas between them (Fig. 6). The elimination of OmpA, one of the most abundant β-barrel proteins, leaves a void in the outer membrane filled by phospholipids (13). Furthermore, in this mutant, lipids phase-separate from β-barrels. Phase separation is expected to lead to a fragile outer membrane due to edge tension at the boundary of domains. Therefore, based on our results we hypothesize that self-affinity between core oligosaccharides, mediated by salt bridges, promotes phase separation in the absence of OmpA, which weakens the outer membrane. In line with this model, we propose that truncation of core oligosaccharides in the *ΔompA* background reduces self-affinity of lipopolysaccharides, leading to outer membrane mixing that increases the stiffness and strength of the outer membrane. In future studies, this model will be interesting to test by directly measuring the effect of mutations to the core-oligosaccharide on outer membrane phase separation. In principle, proteins, phospholipids, and lipopolysaccharides could all separate from one another, depending on their concentrations.

Our model is consistent with a model that was recently proposed to explain the mechanical phenotype of the *ΔbamD* mutant (41). BamD is a regulatory lipoprotein that activates the outer membrane Bam complex (42), which folds β-barrel proteins into the outer membrane. Deletion of *bamD* globally reduces β-barrel content in the outer membrane and, like the deletion of *ompA*, leads to phospholipids in the outer leaflet. It was proposed that

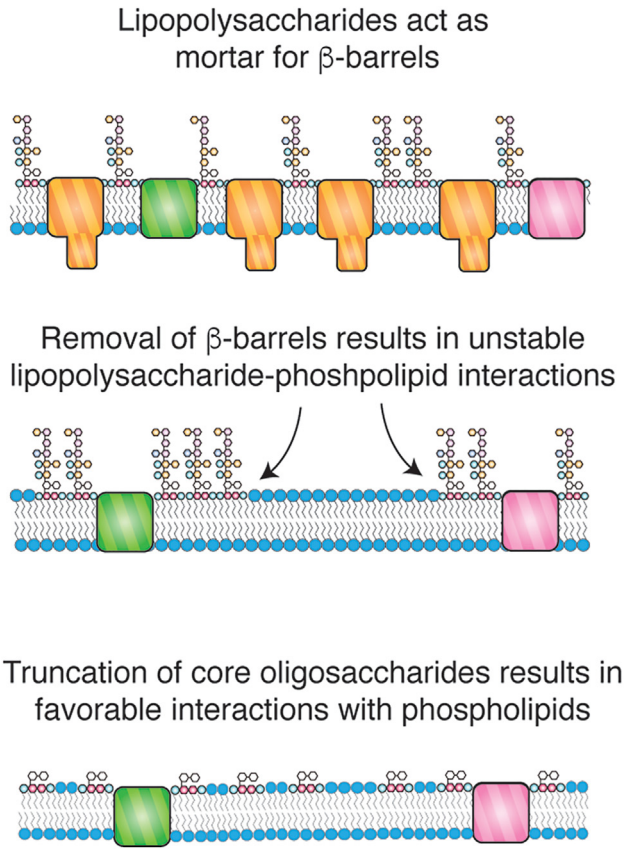

FIGURE 6 Putative model for the effect of the genetic interactions of *ompA* and *waa* genes on cell envelope stiffness.

this leads to surface tension in the outer membrane, which renders the cell fragile to osmotic fluctuations. This was supported by the finding that inhibiting constitutive removal of phospholipids from the outer leaflet by the Mla and PldA systems increases cell viability during fluctuations. Based on our results, we hypothesize that truncating the core oligosaccharide suppresses the mechanical phenotype of *ΔbamD*.

A third key result of our study is that full truncation of core oligosaccharides, deletion of OmpA, and deletion of other outer membrane-cell wall linkers all caused the same quantitative reduction in total cell envelope stiffness (≈20–25%; Figs. 3 *B*, 4 *A*, and 5 *A*). We propose that this convergent phenotype points to a common structural cause for envelope weakening: minor delamination (but not complete detachment) of the outer membrane from the cell wall. In this model, stiffness of the outer membrane plays two related roles: 1) it bears in-plane compression and 2) it prevents out-of-plane buckling (which geometrically limits the outer membrane's ability to bear in-plane compression). This is consistent with our observation that expression of the OmpA β-barrel alone, without the periplasmic linker domain, is sufficient to prevent bulging of the outer membrane upon hyperosmotic shock (Fig. 4, *C*

Please cite this article in press as: Fitzmaurice et al., β-Barrel proteins dictate the effect of core oligosaccharide composition on outer membrane mechanics, Biophysical Journal (2025), https://doi.org/10.1016/j.bpj.2025.01.017

and *D*). It will likely be possible to test this model explicitly by combining the osmotic force-extension assay with super-resolution measurements of outer membrane deformation. An alternative hypothesis for the convergence of the outer membrane stiffness across mutants is that compensatory regulation (e.g., generic upregulation of outer membrane synthesis machinery due to stress-response pathways) inherently limits the degree to which cell-envelope stiffness can be reduced.

Contrary to total envelope stiffness, different perturbations to outer membrane composition had a wide range of effects on outer membrane stiffness (Figs. 3 *C*, 4 *B*, and 5 *B*) when this quantity was decoupled from total envelope stiffness using the plasmolysis-lysis assay. This likely means that these mutations differentially affect the outer membrane's ability to stay mechanically engaged to the cell wall for large hyperosmotic shocks.

Our most surprising result was that modification to lipid A—including those to the headgroup and the acyl chains—had no effect on outer membrane mechanics. Interestingly, this means that divalent cation-mediated bridging of adjacent lipid A moieties has a much greater effect on outer membrane permeability than mechanics.

Collectively, our analysis suggests that the global mechanical properties of the cell envelope arise from complex interactions between the various components of the envelope, rather than additive contributions from each component.

ACKNOWLEDGMENTS

We thank Stephen Trent and Carmen Herrera for helpful discussions and for generously providing the lipid A bacterial mutants. We also thank Georgina Benn for helpful discussions. D.R.F. was funded by an NSF Graduate Research Fellowship DGE-2039655. E.R.R. was supported by NIH grant R35GM143057. G.M.H. was supported by NIH grant R35GM138312.

AUTHOR CONTRIBUTIONS

D.R.F. conceptualized the study, acquired funding, performed microfluidic assays and MD simulations, analyzed data, generated bacterial strains, and wrote the manuscript. A.A. and T.S. performed microfluidic assays, analysis, and bacterial strain generation. G.M.H. conceptualized the study and acquired funding. E.R.R. conceptualized the study, acquired funding, and wrote the manuscript. All authors contributed to discussing the data. D.R.F., G.M.H., and E.R.R. reviewed and edited the manuscript.

DECLARATION OF INTERESTS

The authors declare no competing interest.

SUPPORTING MATERIAL

Supporting material can be found online at https://doi.org/10.1016/j.bpj.2025.01.017.

REFERENCES

1. Rojas, E. R., G. Billings, …, K. C. Huang. 2018. The outer membrane is an essential load-bearing element in Gram-negative bacteria. *Nature.* 559:617–621.
2. Männik, J., R. Driessen, …, C. Dekker. 2009. Bacterial growth and motility in sub-micron constrictions. *Proc. Natl. Acad. Sci. USA.* 106:14861–14866.
3. Yao, Z., D. Kahne, and R. Kishony. 2012. Distinct single-cell morphological dynamics under beta-lactam antibiotics. *Mol. Cell.* 48:705–712.
4. Höltje, J. V. 1998. Growth of the stress-bearing and shape-maintaining murein sacculus of Escherichia coli. *Microbiol. Mol. Biol. Rev.* 62:181–203.
5. Koch, A. L. 1988. Biophysics of bacterial walls viewed as stress-bearing fabric. *Microbiol. Rev.* 52:337–353.
6. Herrmann, M., E. Schneck, …, M. Tanaka. 2015. Bacterial lipopolysaccharides form physically cross-linked, two-dimensional gels in the presence of divalent cations. *Soft Matter.* 11:6037–6044.
7. Rassam, P., N. A. Copeland, …, C. Kleanthous. 2015. Supramolecular assemblies underpin turnover of outer membrane proteins in bacteria. *Nature.* 523:333–336.
8. Ursell, T. S., E. H. Trepagnier, …, J. A. Theriot. 2012. Analysis of surface protein expression reveals the growth pattern of the gram-negative outer membrane. *PLoS Comput. Biol.* 8:e1002680.
9. Raetz, C. R. H., C. M. Reynolds, …, R. E. Bishop. 2007. Lipid A modification systems in gram-negative bacteria. *Annu. Rev. Biochem.* 76:295–329.
10. Needham, B. D., S. M. Carroll, …, M. S. Trent. 2013. Modulating the innate immune response by combinatorial engineering of endotoxin. *Proc. Natl. Acad. Sci. USA.* 110:1464–1469.
11. Wang, X., and P. J. Quinn. 2010. Endotoxins: structure, function and recognition, vol. 53. Springer, pp. 3–25.
12. Schwechheimer, C., A. Kulp, and M. J. Kuehn. 2014. Modulation of bacterial outer membrane vesicle production by envelope structure and content. *BMC Microbiol.* 14:324.
13. Benn, G., I. V. Mikheyeva, …, B. W. Hoogenboom. 2021. Phase separation in the outer membrane of Escherichia coli. *Proc. Natl. Acad. Sci. USA.* 118:e2112237118.
14. Voulhoux, R., M. P. Bos, …, J. Tommassen. 2003. Role of a highly conserved bacterial protein in outer membrane protein assembly. *Science.* 299:262–265.
15. Wu, T., J. Malinverni, …, D. Kahne. 2005. Identification of a multicomponent complex required for outer membrane biogenesis in Escherichia coli. *Cell.* 121:235–245.
16. Mizuno, T., and S. Mizushima. 1990. Signal transduction and gene regulation through the phosphorylation of two regulatory components: the molecular basis for the osmotic regulation of the porin genes. *Mol. Microbiol.* 4:1077–1082.
17. Szmelcman, S., and M. Hofnung. 1975. Maltose transport in Escherichia coli K-12: involvement of the bacteriophage lambda receptor. *J. Bacteriol.* 124:112–118.
18. Doyle, M. T., J. R. Jimah, …, H. D. Bernstein. 2022. Cryo-EM structures reveal multiple stages of bacterial outer membrane protein folding. *Cell.* 185:1143–1156.e13.
19. Mizuno, T. 1981. A novel peptidoglycan-associated lipoprotein (PAL) found in the outer membrane of Proteus mirabilis and other Gram-negative bacteria. *J. Biochem.* 89:1039–1049.
20. Gerding, M. A., Y. Ogata, …, P. A. J. de Boer. 2007. The trans-envelope Tol–Pal complex is part of the cell division machinery and required for proper outer-membrane invagination during cell constriction in E. coli. *Mol. Microbiol.* 63:1008–1025.
21. Braun, V., and H. Wolff. 1970. The murein-lipoprotein linkage in the cell wall of Escherichia coli. *Eur. J. Biochem.* 14:387–391.
22. Cohen, E. J., J. L. Ferreira, …, K. T. Hughes. 2017. Nanoscale-length control of the flagellar driveshaft requires hitting the tethered outer membrane. *Science.* 356:197–200.

23. Schwechheimer, C., C. J. Sullivan, and M. J. Kuehn. 2013. Envelope control of outer membrane vesicle production in Gram-negative bacteria. *Biochemistry.* 52:3031–3040.
24. Deng, Y., M. Sun, and J. W. Shaevitz. 2011. Direct measurement of cell wall stress stiffening and turgor pressure in live bacterial cells. *Phys. Rev. Lett.* 107:158101.
25. Amir, A., F. Babaeipour, …, S. Jun. 2014. Bending forces plastically deform growing bacterial cell walls. *Proc. Natl. Acad. Sci. USA.* 111:5778–5783.
26. Miller, J. H. 1972. Experiments in Molecular Genetics. Cold Spring Habor Lab, pp. 201–205.
27. Datsenko, K. A., and B. L. Wanner. 2000. One-step inactivation of chromosomal genes in Escherichia coli K-12 using PCR products. *Proc. Natl. Acad. Sci. USA.* 97:6640–6645.
28. Rojas, E., J. A. Theriot, and K. C. Huang. 2014. Response of Escherichia coli growth rate to osmotic shock. *Proc. Natl. Acad. Sci. USA.* 111:7807–7812.
29. Jo, S., T. Kim, …, W. Im. 2008. CHARMM-GUI: a web-based graphical user interface for CHARMM. *J. Comput. Chem.* 29:1859–1865.
30. Best, R. B., X. Zhu, …, A. D. Mackerell, Jr. 2012. Optimization of the additive CHARMM all-atom protein force field targeting improved sampling of the backbone ϕ, ψ and side-chain $\chi1$ and $\chi2$ dihedral angles. *J. Chem. Theor. Comput.* 8:3257–3273.
31. Yu, Y., A. Krämer, …, R. W. Pastor. 2021. CHARMM36 lipid force field with explicit treatment of long-range dispersion: parametrization and validation for phosphatidylethanolamine, phosphatidylglycerol, and ether lipids. *J. Chem. Theor. Comput.* 17:1581–1595.
32. Yethon, J. A., E. Vinogradov, …, C. Whitfield. 2000. Mutation of the lipopolysaccharide core glycosyltransferase encoded by waaG destabilizes the outer membrane of Escherichia coli by interfering with core phosphorylation. *J. Bacteriol.* 182:5620–5623.
33. Abraham, M. J., T. Murtola, …, E. Lindahl. 2015. GROMACS: High performance molecular simulations through multi-level parallelism from laptops to supercomputers. *SoftwareX.* 1–2:19–25.
34. 2019. Promoting transparency and reproducibility in enhanced molecular simulations. *Nat. Methods.* 16:670–673.
35. Pagnout, C., B. Sohm, …, J. F. L. Duval. 2019. Pleiotropic effects of rfa-gene mutations on Escherichia coli envelope properties. *Sci. Rep.* 9:9696.
36. Huang, K. C., R. Mukhopadhyay, …, N. S. Wingreen. 2008. Cell shape and cell-wall organization in Gram-negative bacteria. *Proc. Natl. Acad. Sci. USA.* 105:19282–19287.
37. Weinreich, D. M., R. A. Watson, and L. Chao. 2005. Perspective: sign epistasis and genetic costraint on evolutionary trajectories. *Evolution.* 59:1165–1174.
38. Sánchez Carballo, P. M., E. T. Rietschel, …, U. Zähringer. 1999. Elucidation of the structure of an alanine-lacking core tetrasaccharide trisphosphate from the lipopolysaccharide of Pseudomonas aeruginosa mutant H4. *Eur. J. Biochem.* 261:500–508.
39. Booth, I. R., M. A. Jones, …, G. P. Ferguson. 1996. Bacterial ion channels. *Handb. Biol. Phys.* 2:693–729.
40. Bardetti, P., F. Barber, and E. R. Rojas. 2024. Non-linear stress-softening of the bacterial cell wall confers cell shape homeostasis. Preprint at bioRxiv. https://doi.org/10.1101/2024.09.03.611099.
41. Mikheyeva, I. V., J. Sun, …, T. J. Silhavy. 2023. Mechanism of outer membrane destabilization by global reduction of protein content. *Nat. Commun.* 14:5715.
42. Hart, E. M., M. Gupta, …, T. J. Silhavy. 2020. The gain-of-function allele bamA E470K bypasses the essential requirement for BamD in β-barrel outer membrane protein assembly. *Proc. Natl. Acad. Sci. USA.* 117:18737–18743.